Dyes and Pigments 87 (2010) 30–38

Contents lists available at ScienceDirect

Dyes and Pigments

journal homepage: www.elsevier.com/locate/dyepig

# Unsymmetrical squaraine dimer with an extended π-electron framework: An approach in harvesting near infra-red photons for energy conversion

Simon Kuster [a,*], Frédéric Sauvage [b], Md. K. Nazeeruddin [b], Michael Grätzel [b], Frank A. Nüesch [a], Thomas Geiger [a]

[a] Empa, Swiss Federal Laboratories for Materials Testing and Research, Laboratory for Functional Polymers, Überlandstrasse 129, CH-8600 Dübendorf, Switzerland
[b] Laboratoire de Photonique et Interfaces (LPI), Ecole Polytechnique Fédérale de Lausanne (EPFL), CH-1015 Lausanne, Switzerland

ARTICLE INFO

*Article history:*
Received 15 December 2009
Received in revised form
26 January 2010
Accepted 28 January 2010
Available online 14 February 2010

*Keywords:*
Squaraine dye
Dimer
Synthesis
NIR-absorber
Molecular modelling
Dye sensitized solar cell

ABSTRACT

A fully conjugated unsymmetrical dimeric squaraine dye was synthesized. The synthetic key step for this dye, a selective Knoevenagel type condensation of end groups to the core moiety, allows the incorporation of a carboxylic acid function essentially for the strong coupling to the titanium dioxide ($TiO_2$) surface. Moreover, the dimer exhibit outstanding optical properties such as absorption maximum in the NIR region with a huge molar absorption coefficient. The solvatochromic effects were also studied. Furthermore the electrochemical properties were determined with cyclic voltammetry. The reduction potential is just high enough to allow an efficient photo induced charge injection into the conduction band of the $TiO_2$ semiconductor and the oxidation potential lies about 300 mV below the potential of the iodide / triiodide redox couple providing a good regeneration driving force. From electron density distribution calculations of the optimized **BSQ01** structure we could see the directional charge displacement from the solvent exposed side in the HOMO to the carboxyl anchor group in the LUMO. The dimer was immobilised on $TiO_2$ nanoparticles and a first dye sensitized solar cell was made as a proof-of-concept.



## 1. Introduction

Thin film photovoltaic technologies based on the concept of dye sensitized solar cells (DSCs) increasingly emerge as an alternative in solar energy conversion. Over the last decades the consisting need for improved materials led to large efforts in developing highly efficient sensitizers. Mainly ruthenium polypyridyl complexes are used which have reached an overall power conversion efficiency in DSCs to over 11% [1]. Since ruthenium is a rare and expensive element many research groups have considered alternatives, such as replacing ruthenium with copper [2] or by synthesizing metal-free, donor–acceptor dyes [3–5]. As we already published [6,7], small unsymmetrical squaraine dyes **SQ01** and **SQ02** (Scheme 1) were synthesized, which absorb in the far-red domain and feature excellent photon-to-electron conversion efficiencies ($\eta$) in DSCs of up to 5.4%. In order to harvest even more available photons the dyes must display strong absorption in the near-infrared (NIR) region which implies that they must have a very high molar absorption coefficient. The following important requirements should also be fulfilled by all types of sensitizers to achieve high DSC performance: firstly, subsequent to dye excitation, electron injection into the wide band gap semiconductor should be fast and efficient requiring specific electronic properties; secondly, a localized excited state charge density of the dye close to the anchor group attached to the semiconductor surface (titanium dioxide, $TiO_2$) is needed to inject the electrons efficiently; thirdly, the reduction potential (LUMO level) of the dye has to match the $TiO_2$ conduction band edge and finally the oxidation potential (HOMO level) must be high enough to provide the necessary driving force for rapid dye regeneration by the electrolyte redox system.

There are several strategies to shift the absorption of sensitizers into the NIR region. One such possibility was reported by Kiprianov [8] who described a bathochromic shift in polymethine dyes containing two chromophores connected via a conjugated moiety. The shift is explained by the extension of the linear conjugated system. This work describes the implementation of this approach to the formally named squaraine dyes to achieve a fully conjugated unsymmetrical dimeric squaraine dye, **BSQ01** (Scheme 1), with a very high extinction coefficient and absorption maximum in the NIR region. We report on the synthesis, optical and electrochemical properties, electron density calculations and a first proof-of-concept in DSC.

* Corresponding author. Tel.: +41 44 823 55 11; fax: +41 44 823 40 12.
*E-mail address:* simon.kuster@empa.ch (S. Kuster).

0143-7208/$ – see front matter © 2010 Elsevier Ltd. All rights reserved.
doi:10.1016/j.dyepig.2010.01.019

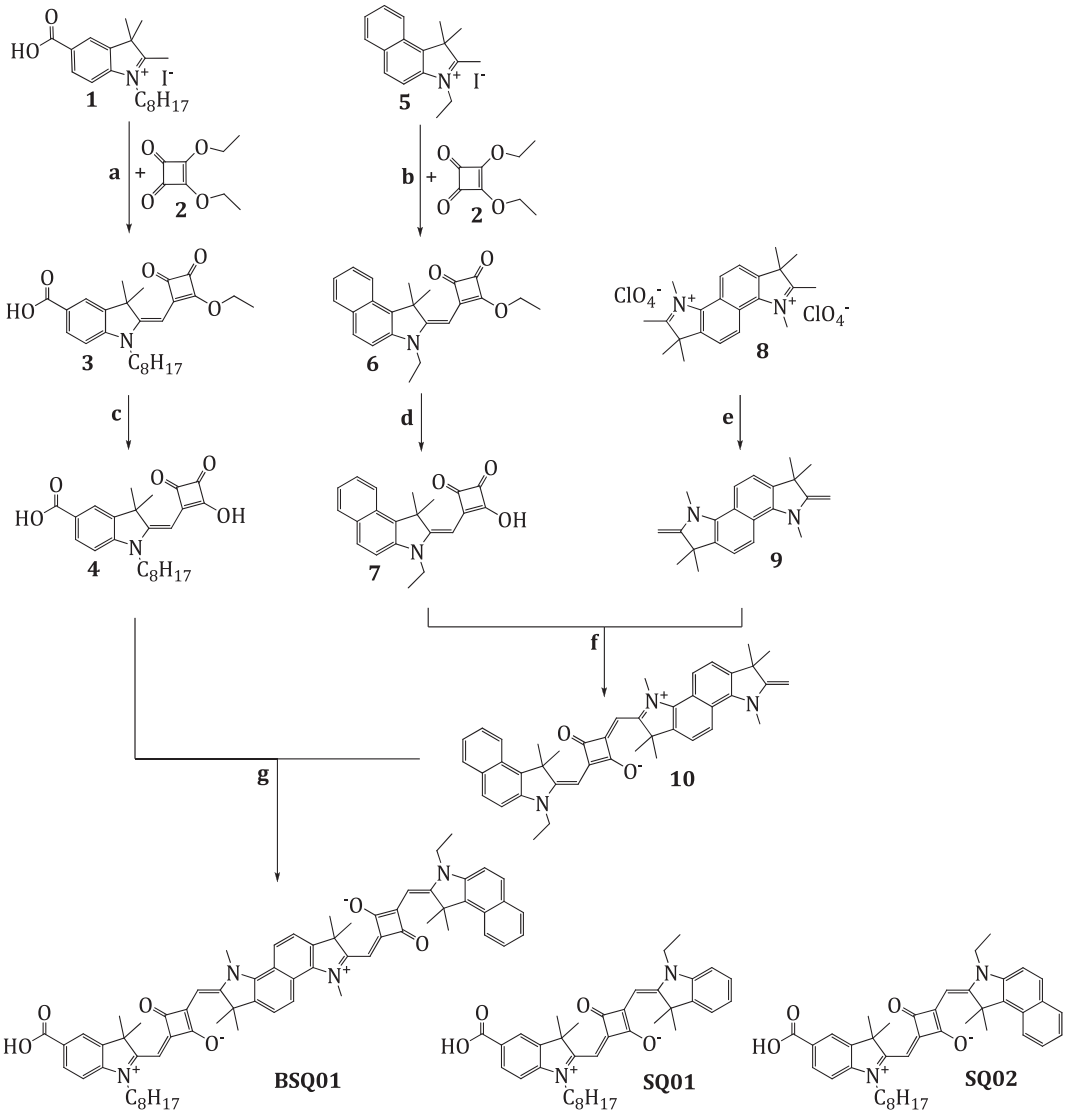


**Scheme 1.** Synthetic strategy for the preparation of the NIR dye **BSQ01** and for comparison the molecular structures of **SQ01** and **SQ02** [6]. Conditions: a) triethylamine (TEA), ethanol, reflux, 15 h; b) TEA, ethanol, reflux, 30 min c) $NaOH_{aq}$. 40% (w/w), ethanol/chloroform (1:1), reflux, 5 min; d) $NaOH_{aq.}$ 40% (w/w), ethanol/chloroform (1:1), reflux, 5 min; e) $NaOH_{aq.}$ (40%, w/w), toluene, room temperature, 30 min; f) quinoline, toluene/1-butanol (1:2), reflux, 16 h; g) quinoline, toluene/1-butanol (1:2), reflux, 72 h.

## 2. Experimental

### 2.1. General information

Unless otherwise stated, reactions were carried out under argon atmosphere, the reaction mixtures being degassed and flushed with argon several times. All condensation reactions were performed in a Dean–Stark apparatus. Analytical thin-layer chromatography (TLC) was performed on glass-baked silica gel with fluorescent indicator (254 nm) obtained from RediSep TM and Fluka. Visualization of the developed TLC was performed under UV (254 and/or 365 nm) either using aq cobalt thiocyanate or aq alkaline potassium permanganate solution. Flash chromatography was performed in a CombyFlash TeledyneISCO system from Companion using RediSep Normal Phase Disposable Columns. Thermogravimetric analysis (TGA) was performed using a Netzsch TG 209 F1 and differential scanning calorimetry (DSC) was undertaken using a Perkin Elmer DSC-7. Nuclear magnetic resonance (NMR) spectra were recorded at 297 K in a 5 mm broadband inverse probe on a Bruker 400 MHz spectrometer. Infra-red (IR) spectra were taken on a Bruker Vector 22 FTIR. Unless otherwise stated, the substances were prepared as KBr pellets or measured as thin film between KBr plates. UV–Vis spectra were recorded on a Varian Cary 50 Scan spectrometer in 1.0 cm optical glass cuvettes. Mass spectra were recorded on a Finnigan TSQ7000 Triple-Quad mass spectrometer (ESI) or on a HiRes-ESI IonSpec Ultima FTMS-spectrometer (Ionspec, Lake Forest, CA, USA). ESI spectra of small organic molecules were usually measured in methanol or dichloromethane. Calculated masses were based on average isotope composition or on single isotope masses for high resolution spectra. Cyclic voltammetry measurements were recorded on a PGStat 30 potentiostat (Autolab) using a three cell electrode system with a rotating glassy carbon working electrode, a platinum counter electrode and an Ag/AgCl (0.1 mol $L^{-1}$ tetrabutylammonium chloride in dimethylformamide (DMF)) reference electrode. **BSQ01** was measured in DMF using 0.1 mol $L^{-1}$ tetrabutylammonium perchlorate (TBAP) as supporting electrolyte; the ferrocene/ferrocenium couple ($Fc/Fc^{+}$) was used as internal reference. The scanning rate of 100 mV $s^{-1}$ and rotation speed of the working electrode was set to 50 rpm. For comparability with the published literature, all

potentials were referenced to normal hydrogen electrode (NHE), by adopting a potential of +0.72 V vs. NHE for $Fc/Fc^+$ in DMF [9]. Fluorescence spectroscopy was carried out on a Fluorolog from Horbia Jobin Yvon with UV–Vis and NIR-Detector.

Compound **8** was synthesized according to Geiger et al. [10]. Compounds **1** and **2** were synthesized according to Yum et al. [7]. Unless otherwise stated, all commercial reagents were used without purification.

### 2.2. Synthesis

#### 2.2.1. 1,1,2,3,6,6,7,8-Octamethyl-1,6-dihydroindolo[7,6-g]indole-3,8-diium diperchlorate (**8**) [10]

Yield: 21% from 1,5-diaminonaphthalene. d.p. 305 °C. $^1$H NMR (DMSO-$d_6$, 400 MHz, ppm): $\delta$ 9.02 (d, $^3J$ = 9.0 Hz, 2H, H-6, H-7), 8.21 (d, $^3J$ = 9.0 Hz, 2H, H-1, H-8), 4.50 (s, 6H, H-17, H-18), 2.91 (s, 6H, H-21, H-22), 1.64 (s, 9H, H-19, H-20, H-23, H-24). For numeration see Supplementary Material. $^{13}$C NMR (DMSO-$d_6$, 100 MHz, ppm): $\delta$ 197.93, 141.93, 137.70, 123.65, 213.35, 122.01, 53.96, 40.38, 20.98, 14.67. MS (ESI-QTOF+): *m/z* 319 (100) $[M-ClO_4-HClO_4]^+$, 223 (5) $[C_{16}H_{17}N]^+$. HR-MS (ESI-QTOF+): *m/z* calculated for: $C_{22}H_{27}N_2$ $[M-ClO_4-HClO_4]^+$ 319.2169; found: 319.2179; $\Delta m/z$ = 1.0 mDa (3.1 ppm). FTIR (KBr, $cm^{-1}$): $\tilde{\nu}$ 3600–3300 (s), 2982 (w), 2938 (w), 2878 (w), 2015 (w), 1619 (m), 1587 (m), 1542 (w), 1470 (m), 1399 (m), 1200–1100 (s), 891 (w), 824 (m), 727 (m), 624 (s).

#### 2.2.2. 5-Carboxy-2,3,3-trimethyl-1-octyl-3H-indolium iodide (**1**) [7]

Yield: 69%. d.p. 201 °C. $^1$H NMR (DMSO-$d_6$, 400 MHz, ppm): $\delta$ 8.39 (s, 1H, H-6), 8.17 (d, $^3J$ = 8.0 Hz, 1H, H-3), 8.10 (d, $^3J$ = 8.0 Hz, 1H, H-2), 4.48 (q, $^3J$ = 6.8 Hz, 2H, H-12), 2.90 (s, 3H, H-22), 1.83 (m, 2H, H-13), 1.58 (s, 6H, H-10, H-11), 1.5–1.2 (m, 12H, H-14, H-15, H-16, H-18, H-19, H-20), 0.84 (t, $^3J$ = 6.0 Hz, 3H, H-21). For numeration see Supplementary Material. $^{13}$C NMR (DMSO-$d_6$, 100 MHz, ppm): $\delta$ 199.43, 166.42, 144.23, 142.26, 131.68, 130.44, 124.42, 115.75, 54.49, 47.97, 31.15, 28.58, 28.47, 27.18, 25.90, 22.02, 21.84, 14.56, 13.94. MS (ESI-QTOF+): *m/z* 442 (2) $[M-H]^+$, 338 (18) $[M-H-I+Na]^+$, 316 (100) $[M-I]^+$. HR-MS (ESI-QTOF+): *m/z* calculated for $C_{20}H_{30}NO_2$ $[M-I]^+$: 316.2271; found: 316.2271; $\Delta m/z$ = 0.0 mDa (0.0 ppm). FTIR (KBr, $cm^{-1}$): $\tilde{\nu}$ 3550 (m), 3479 (m), 3416 (m), 3020 (w), 2958 (m), 2929 (m), 2855 (m), 1721 (s), 1618 (m), 1592 (m), 1468 (m), 1369 (m), 1202 (m),775 (w), 717 (w).

#### 2.2.3. 3-Ethyl-1,1,2-trimethyl-1H-benzo[e]indolium iodide (**5**)

1,1,2-Trimethyl-1*H*-benzo[*e*]indole (100 g, 0.478 mol), iodoethane (100 g, 0.641 mol) and 1-butanol (100 mL) were mixed in a 250 mL Schlenk tube and heated at 80 °C for 8 h. Another portion of iodoethane (40 g, 0.257 mol) was added. After stirring at 80 °C for 16 h, the ensuing reaction mixture was allowed to cool to 40 °C whereupon it was poured into diethyl ether (1 L). The precipitate was filtered and washed with cold diethyl ether several times. The residue was dissolved in boiling chloroform (450 mL) and crystallized by the addition of acetone (2 L) to yield **5** (130 g, 0.35 mol) as white needles. Yield: 73%. d.p. 228 °C. $^1$H NMR (DMSO-$d_6$, 400 MHz, ppm): $\delta$ 8.37 (d, $^3J$ = 8.3 Hz, 1H, H-10), 8.30 (d, $^3J$ = 8.9 Hz, 1H, H-2), 8.22 (d, $^3J$ = 8.0 Hz, 1H, H-1), 8.17 (d, $^3J$ = 8.9 Hz, 1H, H-3), 7.79 (dd, $^3J$ = 7.2, 8.3 Hz, 1H, H-17), 7.72 (dd, $^3J$ = 8.0, 7.2 Hz, 1H, H-18), 4.64 (q, $^3J$ = 7.2 Hz, 2H, H-14), 2.97 (s, 3H, H-10,), 1.76 (s, 6H, H-11, H-12), 1.51 (t, $^3J$ = 7.2 Hz, 3H, H-13). For numeration see Supplementary Material. $^{13}$C NMR (DMSO-$d_6$, 100 MHz, ppm): $\delta$ 195.87, 138.13, 136.95, 132.96, 130.65, 129.65, 128.34, 127.20, 127.16, 123.36, 113.17, 55.40, 43.39, 21.44, 13.84, 12.90. MS (ESI-QTOF+): *m/z* 364 (0.5) $[M-H]^+$, 238 (100) $[M-I]^+$, 223 (1) $[C_{16}H_{17}N]^+$. HR-MS (ESI-QTOF+): *m/z* calculated for $C_{17}H_{20}N$ $[M-I]^+$: 238.1590; found: 238.1601; $\Delta m/z$ = 1.1 mDa (4.6 ppm). FTIR (KBr, $cm^{-1}$): $\tilde{\nu}$ 3550–3250 (w), 3057 (w), 3018 (w), 3001 (w), 2983 (m), 2932 (w), 2907 (w), 2867 (w), 1637 (m), 1618 (w), 1585 (m), 1522 (m), 1464 (m), 1449 (m), 1391 (m), 1366 (m), 1217 (w), 1132 (w), 874 (m), 825 (s), 791 (m), 755 (s), 557 (m), 425 (w).

#### 2.2.4. 3,4-Diethoxycyclobut-3-ene-1,2-dione (**2**)

In a 2 L round bottom flask, squaric acid (100 g, 0.877 mol) and ethanol (1.2 L), followed by triethyl orthoformate (325 g, 2.19 mol) were combined in order to generate **2** after boiling for 20 h. The solvent was evaporated under reduced pressure and the residue was distilled twice under high vacuum (b.p. 82 °C at 0.03 mbar) resulting a colourless liquid of **2** (130 g, 0.75 mol). **CAUTION**: 3,4-diethoxycyclobut-3-ene-1,2-dione can amplify allergic reactions to such an extent that it can cause serious health problems. Yield: 86%. m.p. 13–18 °C. b.p. 245 °C. $^1$H NMR ($CDCl_3$, 400 MHz, ppm): $\delta$ 4.69 (q, $^3J$ = 7.1 Hz, 4H, H-9, H-11), 1.43 (t, $^3J$ = 7.1 Hz, H-1, H-12). For numeration see Supplementary Material. $^{13}$C NMR ($CDCl_3$, 100 MHz, ppm): $\delta$ 189.08, 184.04, 70.37, 15.40. MS (EI+): *m/z* 170 (77) $[M]^+$, 142 (11) $[C_6H_6O_4]^+$, 113 (50) $[C_4HO_4]^+$, 84 (8) $[C_3HO_3]^+$, 57 (17) $[C_2HO_2]^+$, 29 (100) $[C_2H_5]^+$. HR-MS (EI+): *m/z* calculated for $C_8H_{10}O_4$ $[M]^+$: 170.0574; found: 170.0572; $\Delta m/z$ = 0.2 mDa (1.18 ppm). FTIR (film, $cm^{-1}$): $\tilde{\nu}$ 2986 (m), 2938 (w), 1813 (m), 1732 (s), 1599 (s), 1483 (m), 1425 (s), 1383 (m), 1335 (s), 1092 (m), 1026 (s), 801 (m).

#### 2.2.5. 3-Ethoxy-4-((3-ethyl-1,1-dimethyl-1H-benzo[e]indol-2(3H)-ylidene)methyl)cyclobut-3-ene-1,2-dione (**6**)

**5** (50.0 g, 137 mmol), ethanol (150 mL) and triethylamine (22.8 mL, 164 mmol, distilled over potassium hydroxide) were suspended in a 500 mL three neck round bottom flask. While heating to reflux for 30 min the sparingly soluble imminum salt was deprotonated to the soluble enamine form, at which point, the solution was cooled to room temperature and **2** (25.6 g, 151 mmol) was added via a syringe. The reaction mixture was heated at 60 °C for 30 min and the solvent was then evaporated under reduced pressure. To remove triethylamine and unconverted starting materials, the residue was first dried under high vacuum overnight and then suspended in ethanol (50 mL) for 1 h. Subsequently, the suspension was filtered at −5 °C and the residue was washed with cold ethanol (2 × 10 mL). The residue was subsequently dissolved in chloroform (100 mL) and poured into toluene (500 mL) precipitating white triethylammonium iodide which was removed by filtration. After concentration of the filtrate *in vacuo*, side products of blue squaraine dyes were separated by suspension in ethylacetate (50 mL) and subsequent filtration, yielding an orange residue that was recrystallized from hot chloroform/ethanol (1:9) mixture to furnish **6** (44 g, 0.12 mol) as orange hexagonal plates. Yield: 88%. m.p. 186–190 °C. d.p. 276 °C. $^1$H NMR ($CDCl_3$, 400 MHz, ppm): $\delta$ 8.1 (d, $^3J$ = 8.8 Hz, 1H, H-22), 7.87 (d, $^3J$ = 8.4 Hz, 1H, H-25), 7.85 (d, $^3J$ = 8.8 Hz, 1H, H-2), 7.53 (ddd, $^3J$ = 8.8, 7.0 Hz, $^4J$ = 1.4 Hz, 1H, H-23), 7.37 (ddd, $^3J$ = 8.4, 7.0 Hz, $^4J$ = 1.2 Hz, 1H, H-24), 7.22 (d, $^3J$ = 8.8 Hz, 1H, H-3), 5.45 (s, 1H, H-10), 4.93 (q, $^3J$ = 7.0 Hz, 2H, H-13), 4.01 (q, $^3J$ = 7.2 Hz, 2H, H-26), 1.90 (s, 6H, H-11, H-12), 1.56 (t, $^3J$ = 7.0 Hz, 3H, H-14), 1.39 (t, $^3J$ = 7.2 Hz, 3H, H-27). For numeration see Supplementary Material. $^{13}$C NMR ($CDCl_3$, 100 MHz, ppm): $\delta$ 192.70, 187.14, 187.03, 173.26, 169.86, 139.22, 132.58, 130.79, 129.79, 129.60, 128.58, 127.15, 123.73, 122.16, 109.45, 80.48, 69.85, 49.82, 37.80, 26.58, 15.96, 11.68. HR-MS (MALDI): *m/z* calculated for $C_{23}H_{24}NO_3^+$ $[M+H]^+$: 362.1751; found: 362.1753; $\Delta m/z$ = 0.2 mDa (0.55 ppm). FTIR (film, $cm^{-1}$): $\tilde{\nu}$ 3680–3150 (w), 2978 (w), 2932 (w), 1775 (w), 1712 (m), 1619 (s), 1537 (s), 1512 (m), 1416 (m), 1332 (m), 1297 (s), 1253 (s), 1212 (m), 1069 (m), 936 (w), 811 (w).

#### 2.2.6. 3-((3-Ethyl-1,1-dimethyl-1H-benzo[e]indol-2(3H)-ylidene)methyl)-4-hydroxycyclobut-3-ene-1,2-dione (**7**)

In a 500 mL three neck round bottom flask **6** (10.0 g, 27.7 mmol) was dissolved in chloroform (100 mL), the solution was heated to

reflux and aq sodium hydroxide solution (40% w/w) was added via a syringe. After 5 min, the solvent was evaporated under reduced pressure and the remaining mixture was suspended in ethanol (40 mL), cooled to 0 °C, filtered and washed twice with cold ethanol (10 mL). The yellow residue was dissolved in water (500 mL) and acidified with aq saturated citric acid (50 mL) which precipitated the product. To obtain **7** (5.9 g, 17 mmol) as an intensive yellow powder the residue was filtered, washed with water (3 × 15 mL) and dried in a vacuum oven. Yield: 61%. d.p. 92 °C. $^1$H NMR ($CDCl_3$, 400 MHz, ppm): $\delta$ 8.12 (d, $^3J$ = 7.9 Hz, 1H, H-22), 7.88 (m, 2H, H-25, H-2), 7.54 (dd, $^3J$ = 7.9, 7.4 Hz, 1H, H-23), 7.41 (dd, $^3J$ = 8.1, 7.4 Hz, 1H, H-24), 7.27 (d, $^3J$ = 8.0 Hz, 1H, H-3), 5.72 (s, 1H, H-10), 4.10 (q, $^3J$ = 7.1 Hz, 2H, H-13), 1.94 (s, 6H, H-11, H-12), 1.42 (t, $^3J$ = 7.1 Hz, 3H, H-14). For numeration see Supplementary Material. $^{13}$C NMR (DMSO-$d_6$, 100 MHz, ppm): $\delta$ 189.92, 187.99, 176.16, 171.65, 139.01, 133.37, 131.10, 129.73, 128.55, 127.33, 124.21, 122.33, 109.68, 81.56, 50.43, 38.28, 26.60, 11.90. MS (ESI-QTOF+): *m/z* 356 (14) $[M+Na]^+$, 334 (100) $[M+H]^+$, 296 (31), 266 (20), 238 (42), 194 (14) $[C_{14}H_{12}N]^+$. HR-MS (ESI-QTOF+): *m/z* calculated for $C_{21}H_{19}NO_3Na$ $[M+Na]^+$: 356.1257; found: 356.1256; $\Delta m/z$ = 0.1 mDa (0.2 ppm).

### 2.2.7. 2-((2-Ethoxy-3,4-dioxocyclobut-1-enyl)methylene)-3,3-dimethyl-1-octylindoline-5-carboxylic acid (**3**)

**1** (15.0 g, 33.8 mmol) and **2** (7.20 g, 42.3 mmol) were suspended in ethanol (40 mL) and heated to reflux for 15 min. After chilling to 55 °C, triethylamine (11.7 mL, 84.6 mmol) was added. While refluxing for 15 h the colour of the reaction mixture changed from light yellow to dark green. The solvent was distilled under reduced pressure and the residue dried under high vacuum overnight. The residue was then dissolved in chloroform (200 mL), extracted with aq saturated citric acid (2 × 150 mL) and washed with water (3 × 200 mL) and brine (150 mL). The solvent from the combined and dried organic layer was removed under vacuum. The crude product was recrystallized with chloroform/toluene (50:200 mL) to yield **3** (11 g, 25 mmol) as a bright orange solid. Yield: 74%. m.p. 186–192 °C. d.p. 210 °C. $^1$H NMR ($CDCl_3$, 400 MHz, ppm): $\delta$ 8.09 (dd, $^3J$ = 8.3 Hz, $^4J$ = 2.3 Hz, 1H, H-2), 7.97 (d, $^4J$ = 2.3 Hz, 1H, H-6), 6.89 (d, $^3J$ = 8.3 Hz, 1H, H-3), 5.49 (s, 1H, H-10), 4.91 (q, $^3J$ = 7.2 Hz, 2H, H-29), 3.83 (t, $^3J$ = 7.6 Hz, 2H, H-13), 1.75 (m, 2H, H-14), 1.65 (s, 6H, H11, H12), 1.55 (t, $^3J$ = 7.2 Hz, 3H, H-30), 1.5-1.2 (m, 10H, H-15, H-16, H-25, H-26, H27), 0.88 (t, $^3J$ = 6.8 Hz, 3H, H-28). For numeration see Supplementary Material. $^{13}$C NMR ($CDCl_3$, 100 MHz, ppm): $\delta$ 192.1, 188.76, 188.47, 173.68, 171.23, 167.39, 147.52, 140.87, 131.47, 123.85, 122.93, 107.72, 83.27, 70.25, 47.30, 43.16, 31.71, 29.20, 29.09, 27.03, 26.96, 26.33, 22.57, 15.90, 14.06. MS (MALDI): *m/z* 462 (31) $[M+Na]^+$, 440 (100) $[M+H]^+$, 422 (39) $[M+H-H_2O]^+$, 355 (16) $[C_{22}H_{29}NO_3]^+$, 256 (12) $[C_{18}H_{26}N]^+$. HR-MS (MALDI): *m/z* calculated for $C_{26}H_{33}NO_5$ $[M+H]^+$: 440.2432; found: 440.2427; $\Delta m/z$ = 0.5mDa (1.14 ppm). FTIR (KBr, $cm^{-1}$): $\tilde{\nu}$ 3600–3300 (m), 2958 (w), 2929 (m), 2857 (w), 1777 (m), 1721 (m), 1679 (m), 1615 (m), 1603 (m), 1556 (s), 1370 (m), 1304 (m), 1286 (m), 1127 (m), 1056 (w), 936 (w).

### 2.2.8. 2-((2-Hydroxy-3,4-dioxocyclobut-1-enyl)methylene)-3,3-dimethyl-1-octylindoline-5-carboxylic acid (**4**)

In a 500 mL three neck round bottom flask **3** (10.0 g, 22.8 mmol), chloroform (100 mL) and ethanol (100 mL) were mixed and heated to reflux before aq sodium hydroxide solution (5 mL, 40% w/w) was added dropwise via a syringe. Immediately, the colour changed from orange to dark brown and, after 5 min, the reaction mixture was concentrated *in vacuo*. The ensuing black oily residue was dissolved in chloroform (200 mL) and extracted with aq saturated citric acid (200 mL). The protonated product precipitated between the layers of the organic and the aqueous phase and was removed by filtration. Owing to the good water solubility of the product the residue was not washed with pure water; hence, the dried product contained 33% citric acid. **4** (5.50 g, 8.7 mmol) was isolated as orange powder and was immediately used without further purification in the next reaction. Yield: 38%. $^1$H NMR (DMSO-$d_6$, 400 MHz, ppm): $\delta$ 7.86 (m, 2H, H-1, H-5), 7.10 (d, $^3J$ = 8.8 Hz, 1H, H-4), 5.59 (s, 1H, H-17), 3.84 (t, $^3J$ = 6.0 Hz, H-10), 1.61 (m, 2H, H-23), 1.56 (s, 6H, H-11, H-12), 1.4-1.1 (m, 10H, H-24, H-25, H-26, H-27, H-28), 0.80 (t, $^3J$ = 6.2 Hz, 3H, H-29). For numeration see Supplementary Material. MS (ESI-QTOF+): *m/z* 412 (100) $[M+H]^+$, 358 (82), 279 (72), 208 (39), 194 (65), 159 (83). HR-MS (ESI-QTOF+): *m/z* calculated for $C_{24}H_{30}NO_5$ $[M+H]^+$: 412.2118; found: 412.2111; $\Delta m/z$ = 0.7 mDa (1.7 ppm).

### 2.2.9. 4-((3-Ethyl-1,1-dimethyl-1H-benzo[e]indolium-2-yl)methylene)-2-((1,1,3,6,6,8-hexamethyl-7-methylene-7,8-dihydroindolo[7,6-g]indol-2(1H,3H,6H)-ylidene)methyl)-3-oxocyclobut-1-enolate (***10***)

To generate the activated intermediate **9**, a mixture of **8** (3.40 g, 6.55 mmol) in toluene (35 mL) and aq sodium hydroxide solution (10 mL, 40% w/w) was vigorously stirred at room temperature for 30 min. The organic layer was separated and dried with sodium sulfate. Then this layer, **7** (2.20 g, 6.40 mmol), 1-butanol (70 mL) and quinoline (20 mL) as the basic catalyst were combined and heated to reflux overnight. Subsequently, the mixture was poured onto ice (1 L), the precipitate was removed by filtration and the residue was purified using gradual column chromatography (A = ethylacetate/triethylamine/1,1,1,3,3,3-hexafluoroisopropanol = 95:4.9:0.1; B = chloroform/triethylamine/1,1,1,3,3,3-hexafluoroisopropanol = 95:4.9:0.1; gradient A:B = 100:0 to 25:75) to yield **10** (1.9 g, 2.2 mmol). Yield: 35%. d.p. 121 °C. $^1$H NMR (DMSO-$d_6$, 400 MHz, ppm): $\delta$ 8.24 (d, $^3J$ = 8.8 Hz, 1H), 8.17 (d, $^3J$ = 8.8 Hz, 1H), 8.03 (d, $^3J$ = 8.8 Hz, 1H), 8.02 (d, $^3J$ = 8.0 Hz, 1H), 7.93 (d, $^3J$ = 8.8 Hz, 1H), 7.71 (d, $^3J$ = 8.8 Hz, 1H), 7.62 (m, 1H), 7.56 (d, $^3J$ = 8.4 Hz, 1H), 7.46 (t, $^3$J = 7.2 Hz, 1H,), 7.45 (d, $^3J$ = 8.4 Hz, 1H), 5.88 (m, 2H), 4.27 (q, $^3J$ = 7.2 Hz, 2H), 4.14 (d, $^3J$ = 2.0 Hz, 1H), 4.10 (d, $^3J$ = 2.0 Hz, 1H), 4.07 (s, 3H), 1.96 (s, 6H), 1.72 (s, 6H), 1.35 (m, 9H). For numeration see Supplementary Material. $^{13}$C NMR (DMSO-$d_6$, 100 MHz, ppm): $\delta$ 180.90, 177.49, 170.17, 164.15, 142.33, 139.26, 133.34, 132.02, 130.92, 129.83, 129.74, 127.96, 127.45, 124.24, 122.28, 122.22, 120.80, 120.47, 119.39, 118.03, 113.26, 111.16, 104.57, 104.53, 87.17, 85.77, 77.21, 67.27, 66.90, 50.65, 48.35, 45.70, 43.58, 38.25, 35.71, 30.04, 26.53, 26.09, 12.12, 11.75. MS (MALDI): *m/z* 634 (97) $[M+H]^+$, 633 (100) $[M]^+$, 619 (11) $[C_{42}H_{41}N_3O_2]^+$, 411 (6) $[C_{27}H_{26}N_2O_2]^+$, 317 (5) $[M+H]^{++}$. HR-MS (MALDI): *m/z* calculated for $C_{43}H_{43}N_3O_2$ $[M]^+$: 633.3350; found: 633.3351; $\Delta m/z$ = 0.1 mDa (1.74 ppm). FTIR (KBr, $cm^{-1}$): $\tilde{\nu}$ 3600–3300 (m), 2965 (w), 1587 (m), 1494 (s), 1460 (m), 1432 (w), 1282 (s), 1250 (m), 1207 (s), 1122 (m), 1063 (m), 986 (m), 935 (m).

### 2.2.10. 2-((5-Carboxy-3,3-dimethyl-1-octylindolin-2-ylidene)methyl)-4-((7-((3-((3-ethyl-1,1-dimethyl-1H-benzo[e]indol-2(3H)-ylidene)methyl)-2-oxido-4-oxocyclobut-2-enylidene)methyl)-1,1,3,6,6,8-hexamethyl-1,6-dihydroindolo[7,6-g]indol-3,8-diium-2-yl)methylene)-3-oxocyclobut-1-enolate (***BSQ01***)

**10** (1.50 g, 1.77 mmol), **4** (1.29 g, 1.84 mmol), toluene (15 mL), 1-butanol (30 mL) and quinoline (1 mL) were combined in a 100 mL round bottom flask. The reagents were refluxed for three days after which the ensuing mixture was cooled to room temperature and poured onto ice (1 L). The precipitate was filtered and dissolved in chloroform (200 mL). The organic layer was extracted with water (3 × 200 mL) and aq saturated potassium carbonate solution (200 mL). The resulting potassium salt of the product precipitated between the two phases and was separated by centrifugation. The residue was washed several times with water and dried. The fine powder was suspended in an aq saturated citric acid solution and

extracted with chloroform. The organic solvent was evaporated under vacuum to yield **BSQ01** (0.36 g, 0.35 mmol) as dark blue powder. Yield: 19%. d.p. 273 °C. $^1$H NMR (DMSO-$d_6$, 400 MHz, ppm): $\delta$ 8.39 (d, $^3J = 9.2$ Hz, 1H, H-7), 8.34 (d, $^3J = 8.8$ Hz, 1H, H-6), 8.26 (d, $^3J = 8.2$ Hz, 1H, H-45), 8.05 (d, $^3J = 9.0$ Hz, 1H, H-26), 8.03 (d, $^3J = 7.2$ Hz, 1H, H-48), 8.00 (d, $^4J = 1.4$ Hz, 1H, H-49), 7.94 (dd, $^3J = 8.6$ Hz, $^4J = 1.4$ Hz, 1H, H-53), 7.78 (d, $^3J = 8.8$ Hz, 1H, H-1), 7.77 (d, $^3J = 9.4$ Hz, 1H, H-8), 7.75 (d, $^3J = 9.0$ Hz, 1H, H-27), 7.63 (dd, $^3J = 8.2$, 7.6 Hz, 1H, H-46), 7.47 (dd, $^3J = 7.6$, 7.2 Hz, 1H, H-47), 7.36 (d, $^3J = 8.6$ Hz, 1H, H-52), 6.0–5.85 (m, 4H, H-21, H-22, H-34, H-65), 4.31 (q, $^3J = 6.8$ Hz, 2H, H-37), 4.15–4.05 (m, 8H, H-17, H-18, H-58), 1.96 (s, 6H, H-35, H36), 1.74 (s, 12H, H-19, H-20, H-23, H-24), 1.70 (s, 6H, H-59, H-60), 1.74–1.70 (m, 2H, H-71), 1.40–1.20 (m, 13H, H-38, H-72, H-73, H-74, H-75, H-76), 0.85 (t, $^3J = 6.4$ Hz, 3H, H-77). For numeration see Supplementary Material. $^{13}$C NMR (DMSO-$d_6$, 100 MHz, ppm): $\delta$ 181.10, 181.02, 180.89, 180.76, 177.70, 176.72, 173.17, 171.15, 167.86, 167.12, 146.24, 141.26, 139.12, 138.91, 138.71, 138.31, 133.76, 131.09, 130.28, 129.93, 129.76, 127.90, 127.53, 125.22, 124.47, 123.13, 122.38, 122.08, 121.78, 120.16, 119.64, 118.26, 111.30, 109.67, 104.58, 88.10, 87.56, 87.28, 86.16, 50.91, 48.89, 48.17, 48.10, 42.98, 40.19, 38.48, 37.50, 31.15, 28.67, 28.59, 26.67, 26.66, 26.44, 26.43, 26.19, 26.17, 26.00, 22.06, 13.96, 12.21. MS (MALDI): *m/z* 1050 (3) $[M+Na]^+$, 1028 (100) $[M+H]^+$, 1027 (64) $[M]^+$, 1012 (16) $[M-CH_3]^+$, 997 (5) $[M-CH_2CH_3]^+$,983 (1) $[M-CO_2]^+$, 915 (1) $[C_{59}H_{55}N_4O_6]^+$, 804 (2) $[C_{51}H_{54}N_3O_6]^+$, 726 (1) $[C_{48}H_{44}N_3O_4]^+$, 709 (3) $[C_{46}H_{51}N_3O_4]^+$, 697 (2) $[C_{45}H_{51}N_3O_4]^+$, 619 (1) $[C_{42}H_{41}N_3O_2]^+$, 514 (4) $[M+H]^{++}$, 408 (1) $[C_{25}H_{30}NO_4]^+$, 330 (2) $[C_{22}H_{20}NO_2]^+$, 257 (1) $[M+H]^{4+}$. HR-MS (MALDI): *m/z* calculated for $C_{67}H_{71}N_4O_6$ $[M+H]^+$: 1027.5368; found: 1027.5386; $\Delta m/z = 1.8$ mDa (1.75 ppm). FTIR (KBr, cm$^{-1}$): $\tilde{\nu}$ 3554 (m), 3478 (m), 3415 (m), 3234 (w), 2961 (w), 2929 (w), 2861 (w), 1709 (w), 1638 (w), 1614 (m), 1492 (s), 1458 (w), 1432 (w), 1363 (m), 1277 (s), 1206 (s), 1096 (s), 1066 (m), 1048 (m), 985 (m), 836 (m), 679 (w), 606 (w), 464 (w). UV–Vis (DMF, nm (L mol$^{-1}$ cm$^{-1}$)): $\lambda_{abs}$ (log $\varepsilon$) 579 (4.27), 633 (4.86), 682 (5.19), 730 (5.59). Fluorescence (DMF, nm): $\lambda_{em}$ 746, 807, 842.

### 2.3. Molecular modelling

The structure and electron density contribution of the dimer **BSQ01** was studied with DFT calculations using NWChem 5.1 program [11, 12] on the Ipazia computing cluster at Empa. Analysis of NWChem log-files and illustrations of the calculated frontier dye orbitals were performed by the program Jmol, an open-source Java viewer for chemical structures [13].

### 2.4. Solar cell preparation

#### 2.4.1. Device fabrication

A screen-printed double layer thick film of interconnected titanium dioxide ($TiO_2$) particles was used as photo-anode upon NSG10 TCO glass (Nippon Sheet Glass). The first 8 μm thick and optically transparent layer was composed of 20 nm particles of anatase $TiO_2$. A second 5 μm thick layer, based on 400 nm size particles, was used to backscatter the unabsorbed photons towards the dye. The cells were dye loaded in $10^{-5}$ mol L$^{-1}$ diluted solution of **BSQ01** in chloroform overnight. 3α,7α-Dihydroxy-5β-cholanic acid (CDCA) was used as de-aggregating agent in different proportions from 0 to 40 mol mol$^{-1}$ during cell optimization. After being washed by acetonitrile and dried in water free air box, the derivatized electrodes were separated by a 25 μm thick Surlyn gasket melt by heating with the Pt-modified TEC15 TCO. This latter was prepared by spreading out a drop of 5 mmol L$^{-1}$ $H_2PtCl_6$ in ethanol solution before heating the counter electrode at 400 °C during 15 min under air. The internal space between the two electrodes was filled with M1 electrolyte using a vacuum back filling system. The hole, priorly made by sand-blasting, was clogged-up with a melted Bynel sheet. The volatile M1 electrolyte is composed by 0.6 mol L$^{-1}$ 1-butyl-3-methylimidazolium iodide (BMII), 50 mmol L$^{-1}$ LiI, 40 mmol L$^{-1}$ $I_2$, 0.275 mol L$^{-1}$ tert-butylpyridine and 0.05 mol L$^{-1}$ GuNCS in a solvent mixture of 85% acetonitrile with 15% valeronitrile by volume. Anti-reflecting coating on the NSG10 glass was also used to prevent incident light losses. An aluminium foil at the back side of the counter electrode was taped to reflect unabsorbed light back to the photo-anode. The thickness of the electrodes was evaluated by profilometry.

#### 2.4.2. Photovoltaic and cell characterization

A 450 W xenon light source (Oriel, USA) was used to provide an incident irradiance of 100 mW cm$^{-2}$ at the surface of the solar cells. The spectral output of the lamp was filtered using Schott K113 Tempax sunlight filter (Präzisions Glas & Optik GmbH, Germany) to reduce light mismatch between real solar illumination and the simulated one to less than 2%. Light intensities were regulated with wire mesh attenuators. The J-V measurements were performed using a Keithley model 2400 digital source meter (Keithley, USA) by applying independently external voltage to the cell and by measuring the photo-generated current out from the cell. Incident photon-to-current conversion measurements were realized using a 300 W xenon light source (ILC Technology, USA). A Gemini-180 double monochromator Jobin Yvon Ltd. (UK), was used to select and increment wavelength irradiation to the cell.

## 3. Results and discussion

### 3.1. Synthesis

The synthetic strategy of **BSQ01** is shown in Scheme 1. Indole derivatives **4** and **7** were synthesized similarly starting with a Knoevenagel-type condensation reaction of the alkylated indolium derivative **1** [7] and **5** [6], respectively, with the squaric acid diethyl ester **2** [7] followed by a basic ester cleavage and protonation. For the unsymmetric structure of **BSQ01** it was essential to condense one indole derivative **7** to the core moiety **9** to yield squaraine dye **10**. This was enabled because the hardly soluble naphthalene derivative **8** [10] was deprotonated to the core moiety **9**, which was well soluble in toluene. Subsequently, the last Knoevenagel-type condensation of indole derivative **4** to the squaraine dye **10** yielded the desired dimer **BSQ01**.

### 3.2. Optical properties

Due to the extended linear π-framework and the implemented planarity of the naphthalene moiety of the new NIR-absorber the absorption maximum ($\lambda_{max}$) shifted as expected batochromically by 70–80 nm in comparison to **SQ01** or **SQ02** [6] (Table 1, Fig. 1). The massive increase of the molar absorption coefficient ($\varepsilon$) to 389000 L mol$^{-1}$ cm$^{-1}$ reflects the two chromophore units present in the dimer. Due to the coupling of the two **BSQ01** dye systems the absorption bands are split and the UV–Vis spectrum shows an

**Table 1**
Optical data of **BSQ01** compared to **SQ01** and **SQ02** [6] (DMF).

| Entry | $\lambda^{abs}_{max}$ [nm] | $\varepsilon$ ($\lambda^{abs}_{max}$) [L mol$^{-1}$ cm$^{-1}$] | $\lambda^{em}_{max}$ [nm] | $\lambda_s$ [nm] | $\lambda_{onset}$ [nm] | $\Delta E_{opt}$ [eV] |
|---|---|---|---|---|---|---|
| **SQ01** | 647 | 292000 | 661 | 14 | 669 | 1.85 |
| **SQ02** | 662 | 319000 | 674 | 12 | 684 | 1.81 |
| **BSQ01** | 730 | 389000 | 745 | 15 | 754 | 1.64 |

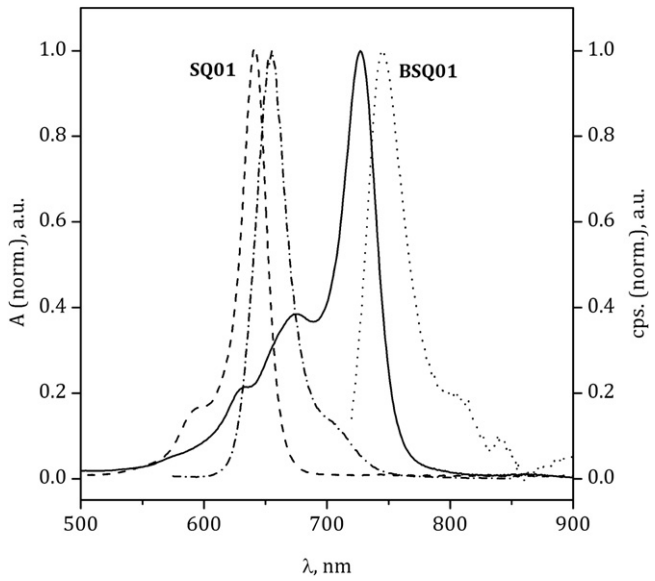


**Fig. 1.** Normalized UV–Vis absorption of **SQ01** in DMF (dashed line) and of **BSQ01** in DMF (solid line) and the emission spectrum of **SQ01** (dash-dotted line) and of **BSQ01** (dotted line).

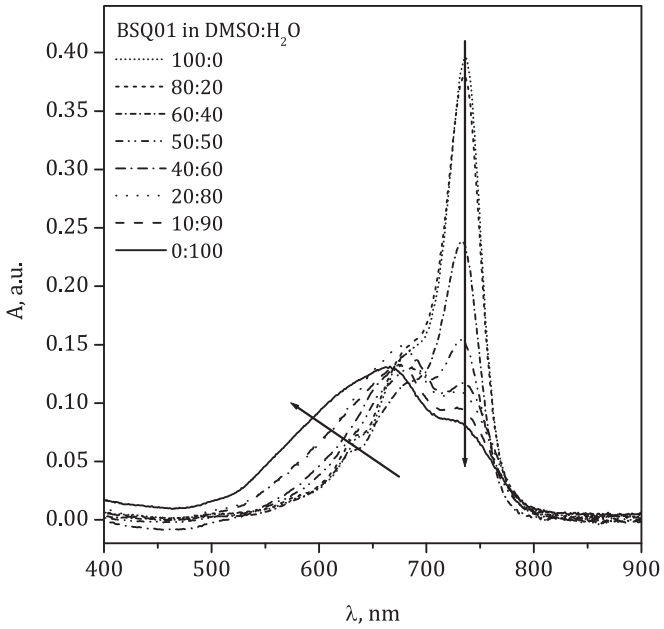


**Fig. 3.** UV–Vis absorption spectrum of **BSQ01** in DMSO-water mixtures.

intense long-wavelength band (730 nm with shoulder at 678 nm) and a weak short-wavelength band (635 nm with shoulder at 578 nm). This behaviour was also reported by Kiprianov [8], demonstrating the influence of the coupling between two dependent dye moieties on the absorption spectrum. The optical band gap ($\Delta E_{opt}$) of 1.64 eV was calculated from the onset in the absorption spectrum of **BSQ01** in dimethylformamide (DMF). A small Stokes shift ($\lambda_s$) of 15 nm was measured indicative of similar molecular configurations in the ground and excited state.

Since the squaraine dye class is known for its solvatochromic effects [14, 15], the solvatochromic shift of **BSQ01** was studied using 17 solvents. A rather small sovlatochromy of 42 mV or 18 nm was detected between the lowest influencing methyl *tert*-butyl ether (MTBE) and highest influencing dimethylsulfoxide (DMSO). Nevertheless three solvent groups could be determined which had an almost perfect proportional correlation between the absorption maximum energy ($\Delta E_{max}$) of **BSQ01** and the dielectric constant ($\varepsilon_s$) of the solvent (Fig. 2): Solvents containing an aromatic system showed the strongest and the most linear influence probably due to strong π–π interactions; Solvents containing an oxygen atom showed a very good correlation over a wide range which is most likely due to interactions with the π-system and hydrogen bounding with the anchoring group; Solvents containing neither an aromatic system nor an oxygen atom showed a rather weak solvent

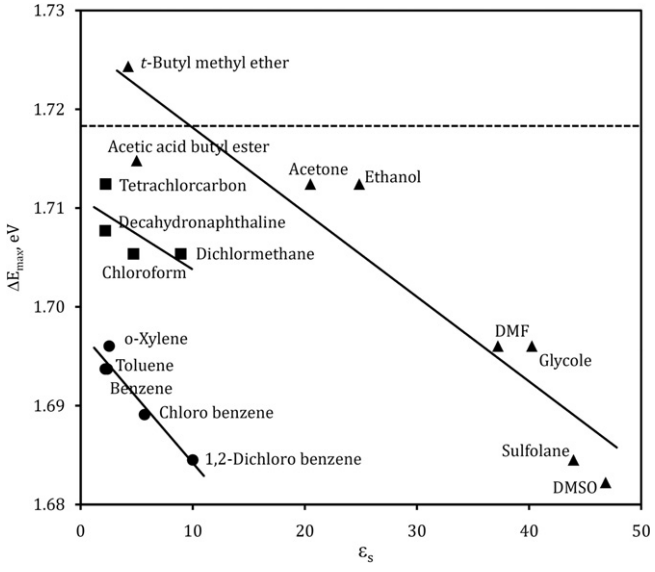


**Fig. 2.** Correlation of the maximum absorption energy ($\Delta E_{max}$) of **BSQ01** with the solvent dielectric constant ($\varepsilon_s$). $\Delta E_{max}$ of the immobilized dye on titanium dioxide (dashed line). The three solvent groups: oxygen atom containing solvents (triangular dots), aromatic system containing solvents (circular dots) and solvents containing neither an oxygen atom nor an aromatic system (squaric dots).

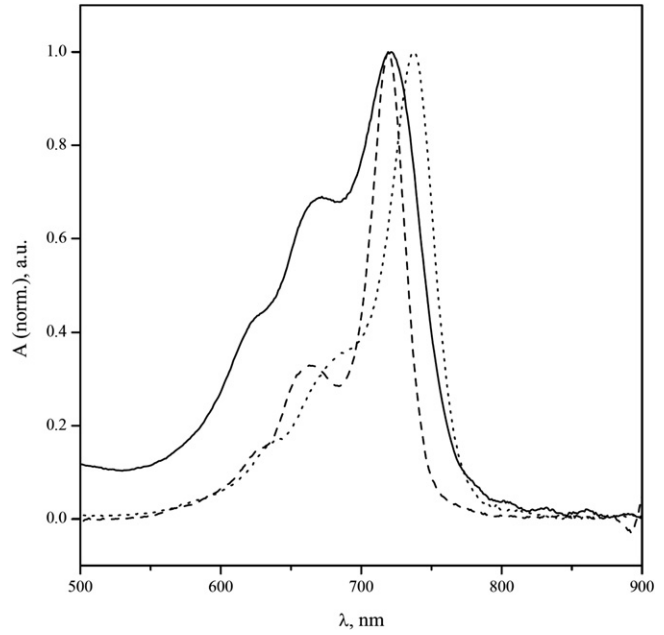


**Fig. 4. BSQ01** immobilized on $TiO_2$ surface against air (solid line), dissolved in MTBE (dashed line) and dissolved in DMSO (dotted line).

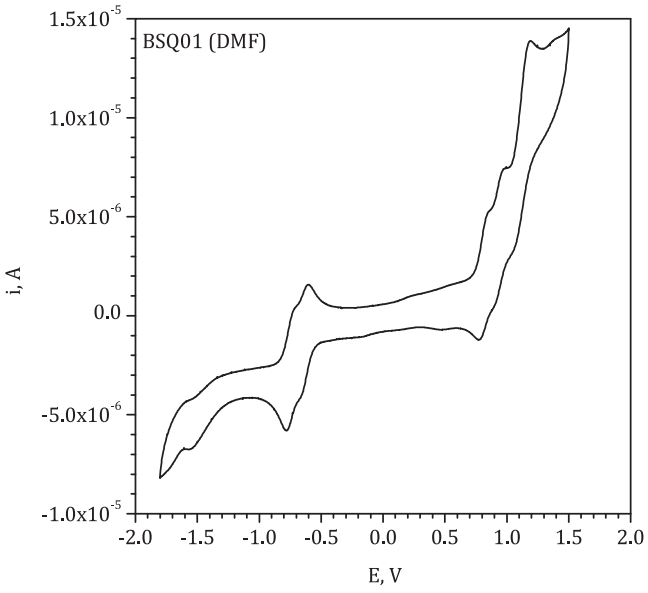


**Fig. 5.** Cyclic voltammogram of dimer **BSQ01** measured in DMF.

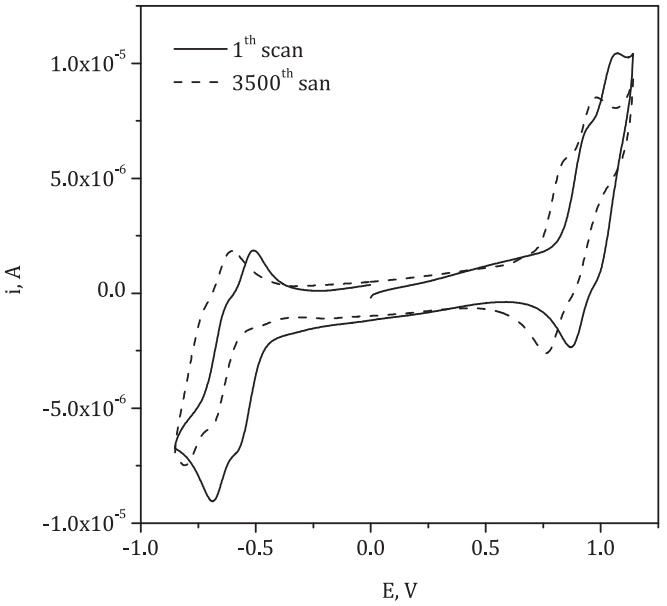


**Fig. 6.** Long-term electrochemical stress experiment of dimer **BSQ01** measured in DMF. Cyclic voltammograms of the first and the 3500th scan after 24 h are provided.

polarity influence on the absorption maximum which was to be expected. Despite the increase of solvent polarity with DMSO–water mixtures, the absorption was not further red shifted as expected, but blue-shifted due to aggregation of the dye (Fig. 3). The so formed aggregates, presumably *H*-aggregates [16,17], showed a very broad absorption band at 652 nm while the typical sharp and intense main transition peak disappeared almost completely.

In order to determine the absorption spectrum of **BSQ01** on $TiO_2$ surface, a half cell was dipped in a $3 \times 10^{-6}$ M dye solution in chloroform for 6 h, then washed with fresh chloroform and measured straight afterwards. The UV–Vis spectra is displayed in comparison with the solution spectra in MTBE and DMSO (Fig. 4). The peak is quite broad but still shows all of the features as a spectrum in solution. Due to the very polar surface one would expect that the absorption maximum of the immobilized dye is close to the one in DMSO but MTBE, acetic acid butyl ester, tetrachlorcarbon, acetone or ethanol (Fig. 2) describe the environment much better.

### 3.3. Electrochemical properties

Cyclic voltammetry measurements were performed in DMF solution using 0.1 mol $L^{-1}$ tetrabutylammonium perchlorate as the supporting electrolyte. Ferrocene was used as internal standard of which oxidation potential was set to 0.72 V vs. NHE [9]. The cyclic voltammogram of the dimer **BSQ01** showed sharp, reversible oxidation and reduction waves (Fig. 5). The reversibility was proven by determining the ratio of each cathodic and anodic peak current ($i_{pa}/i_{pc}$) which approached unity in all cases (details are not shown here). Since the Stockes shift is small, the redox potentials can be approximated as the HOMO and LUMO levels and were calculated at −0.73 V and +0.73 V, respectively, versus NHE [9], leading to a fairly low electronic band gap ($\Delta E_{el}$) of 1.46 eV. Particularly with regard to an application in DSCs and given the position of the $TiO_2$ conduction band edge lying at about −0.5 V vs. NHE and $I_3^-/I^-$ redox potential at about +0.4 V vs. NHE, the redox potentials of **BSQ01** are perfectly positioned with 230 mV driving force for electron injection and 330 mV overpotential for dye regeneration.

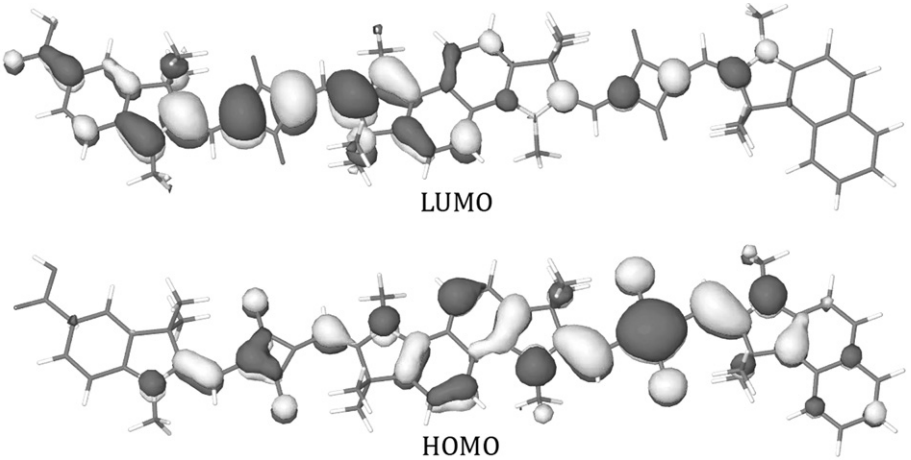


**Fig. 7.** Calculated frontier molecular orbitals of **BSQ01**.

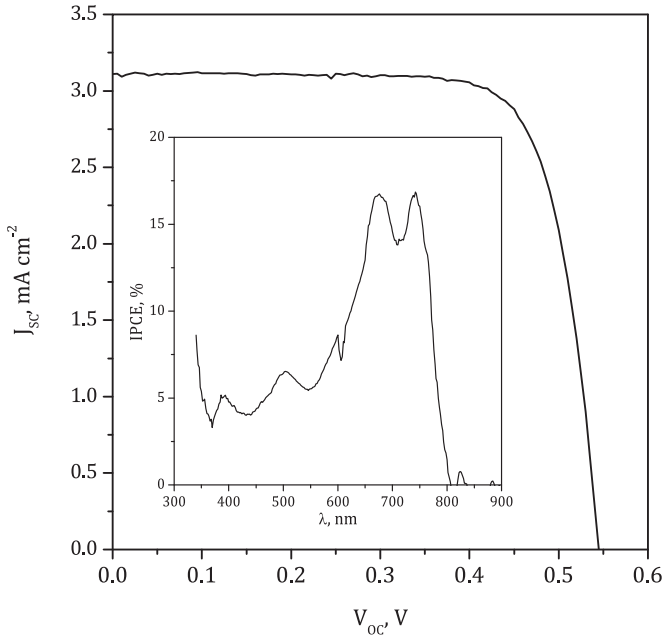


**Fig. 8.** Photocurrent action spectrum (insert) and current-voltage characteristics of a **BSQ01** sensitized solar cells.

For inferring the electrochemical stability of the NIR dye, long-term cyclic voltammetry measurements were performed by accomplishing 3500 full cycles up to 1.15 V and down to −0.85 V within 24 h. The first and last scan is shown in Fig. 6. Importantly, the electrochemical band gap of **BSQ01** remained unchanged after 3500 scans, albeit the diffusion processes of chloride ions out of the reference electrode shifted all potentials towards lower voltage. Also during the one day measurement neither an additional oxidation nor reduction peak appeared implying that the dye is indeed electrochemically stable under applied experimental conditions.

### 3.4. Analysis of the dye structure – molecular modelling

As mentioned above, one of the basic requirements for an efficient sensitizer is a localized excited state charge density of the dye close to the anchor group attached to the semiconductor surface which allows an efficient vectorial electron transfer from the light-harvesting dye towards the semiconductor surface. So as to prove that, optimized molecular structures for **BSQ01** were calculated in which for the sake of time the alkyl chains were reduced to methyl units. To additionally visualize the frontier orbitals, electron density distribution of the optimized **BSQ01** structure was calculated using Density Functional Theory (DFT) with B3LYP functional and 6-31G* as the basis set. The LUMO is located at the dye moiety containing the anchoring carboxylic acid group, whereas the HOMO is situated on the opposite side (Fig. 7). This implies directional charge transfer to the carboxyl anchoring group upon photo-excitation.

### 3.5. Preparation of dye sensitized solar cells

Finally, a DSC was prepared by using a low concentrated dye solution ($10^{-5}$ mol $L^{-1}$) in chloroform. CDCA was used to prevent formation of aggregates on the $TiO_2$ surface [6, 7]. The evolution of the "incident photon-to-current-conversion efficiency" (IPCE) curve as a function of the molar ratio of CDCA rising from 0 to 40 mol/mol was investigated where the best performance was obtained at the highest CDCA ratio. At this stage, our device data rather serve to proof the concept than to rate the potential of squaraine dyes for DSC applications. The cell showed a short circuit current density ($J_{sc}$) of 3.11 mA cm$^{-2}$, an open circuit voltage ($V_{oc}$) of 545 mV and a fill factor (ff) of 0.76 leading to $\eta$ of 1.3% obtained under 100 mW cm$^{-2}$ illumination intensity. We could clearly demonstrate that photocurrent is produced from 550 nm up to 800 nm where **BSQ01** absorbs (Fig. 8). Although, the IPCE curve did not precisely follow the UV–Vis spectrum but presents mainly two bands situated at 675 nm and 742 nm. An explanation for the former peak might be aggregate formation, similar to that shown in Fig. 4, albeit CDCA was used in the cell preparation. We postulate the appearance of these *H*-aggregates, which were known to quench excited states, as the reason for the low device performance. A tuning with different anti aggregating agents and a modification in the molecular structure should certainly lead to non aggregated dye absorption and therefore also to higher cell performance.

## 4. Conclusions

In summary, a fully conjugated metal-free unsymmetrical dimeric squaraine dye (**BSQ01**) was straightforwardly synthesized. The key step in the synthesis was the stepwise Knoevenagel-type condensation of indole derivatives **4** and **7** to the naphthalene moiety **9**. Due to the distinctive design the dimer absorbs in the far-red and in the NIR region. Therefore, **BSQ01** has the basic requirements to function as a sensitizer in a DSC, namely: A localized excited state charge density upon the anchoring group (visualized by molecular modelling), the optimal positioned redox levels to fit those of the $TiO_2$ conducting band edge and the $I_3^-/I^-$ electrolyte redox potential (demonstrated by CV measurements), the ability to harvest NIR photons for energy conversion (proven by the DSC characterization) and finally the huge extinction coefficient which allows the use of even thinner $TiO_2$ nano particle layers and also substantially reduces the amount of immobilized sensitizer. This work paves the way for designing new NIR-absorbers for DSC and organic photovoltaic devices. Further efforts to improve the actual **BSQ01**-based DSC performance by using high efficient anti aggregation agents and changes in molecular design towards bulkier side chains are underway.

## Acknowledgements

B. Fischer is kindly acknowledged for DSC-TGA measurements and the MS service at the ETH Zürich for MS analysis. NWChem Version 5.1, as developed and distributed by Pacific Northwest National Laboratory, P. O. Box 999, Richland, Washington 99352 USA, and funded by the U. S. Department of Energy, was used to obtain some of these results. FS, MKN and MG thank the Swiss Federal Office for Energy (OFEN) for the financial support. SK, FAN and TG thank the Swiss Federal Laboratories for Materials Testing and Research for the financial support.

## Appendix. Supplementary data

Supplementary data associated with article can be found in the online version at doi:10.1016/j.dyepig.2010.01.019.

## References

[1] Chiba Y, Islam A, Wanatabe Y, Komiya R, Koide N, Han L. Dye-sensitized solar cells with conversion efficiency of 11.1%. Japanese Journal of Applied Physics 2006;45:L638–40.
[2] Bessho T, Constable EC, Grätzel M, Redondo AH, Housecroft CE, Kylberg W, et al. An element of surprise—efficient copper-functionalized dye-sensitized solar cells. Chemical Communications; 2008:3717–9.
[3] Mishra A, Fischer MKR, Bäuerle P. Metal-free organic dyes for dye-sensitized solar cells: from structure: property relationships to design rules. Angewandte Chemie International Edition 2009;48:2474–99.

[4] Ooyama Y, Harima Y. Molecular designs and syntheses of organic dyes for dye-sensitized solar cells. European Journal of Organic Chemistry 2009;2009:2903–34.
[5] Ning Z, Zhang Q, Wu W, Pei H, Liu B, Tian H. Starbust triarylamine based dyes for efficient dye-sensitized solar cell. Journal of Organic Chemistry 2008; 73:3791–7.
[6] Geiger T, Kuster S, Yum J, Moon S, Nazeeruddin MK, Grätzel M, et al. Molecular design of unsymmetrical squaraine dyes for high efficiency conversion of low energy photons into electrons using $TiO_2$ nanocrystalline films. Advanced Functional Materials 2009;19:2720–7.
[7] Yum J, Walter P, Huber S, Rentsch D, Geiger T, Nüesch F, et al. Efficient far red sensitization of nanocrystalline $TiO_2$ films by an unsymmetrical squaraine Dye. Journal of the American Chemical Society 2007;129:10320–1.
[8] Kiprianov AI. Absorption spectra of organic dyes containing two chromophores. Russian Chemical Reviews 1971;40:594–607.
[9] Bard AJ. Electrochemical methods: fundamentals and applications. New York: Wiley; 2001.
[10] Geiger T, Benmansour H, Fan B, Hany R, Nüesch F. Low-band gap polymeric cyanine dyes absorbing in the NIR region. Macromolecular Rapid Communications 2008;29:651–8.
[11] Straatsma TP, Aprà E, Windus TL, Bylaska EJ, de Jong W, Hirata S, et al. NWChem, a computational chemistry package for parallel computers, Version 4.6. Richland, Washington 99352-0999, USA: Pacific Northwest National Laboratory; 2004.
[12] Kendall RA, Aprà E, Bernholdt DE, Bylaska EJ, Dupuis M, Fann GI, et al. High performance computational chemistry: an overview of NWChem a distributed parallel application. Computer Physics Communications 2000;128:260–83.
[13] http://www.jmol.org.
[14] Mishra A, Behera RK, Behera BK, Mishra BK, Behera GB. Cyanines during the 1990s: a review. Chemical Reviews 2000;100:1973–2011.
[15] Berezin MY, Lee H, Akers W, Achilefu S. Near infrared dyes as lifetime solvatochromic probes for micropolarity measurements of biological systems. Biophysical Journal 2007;93:2892–9.
[16] Neumann B, Pollmann P. Investigation of two cyanine dyes at normal and high pressure by UV/Vis spectroscopy. Physical Chemistry Chemical Physics 2000;2:4784–92.
[17] Kim S, Kim J, Cui J, Gal Y, Jin S, Koh K. Absorption spectra, aggregation and photofading behaviour of near-infrared absorbing squarylium dyes containing perimidine moiety. Dyes and Pigments 2002;55:1–7.